RSC Advances

ROYAL SOCIETY OF CHEMISTRY

www.rsc.org/advances

Synthesis of fluorescent nitrogen-doped carbon dots from dried shrimps for cell imaging and boldine drug delivery system†

Stephanie L. D'souza[a], Balaji Deshmukh[b], Jigna R. Bhamore,[a] Karuna A. Rawat[a], Nibedita Lenka[b] and Suresh Kumar Kailasa[a*]

[a]Department of Chemistry, S. V. National Institute of Technology, Surat – 395007, Gujarat, India.
[b]National Center for Cell Science, NCCS Complex, Pune University Campus, Pune- 411 007, Maharastra, India.
[*]Corresponding author, Phone: +91-261-2201730; Fax: +91-261-2227334
E-mail: sureshkumarchem@gmail.com; skk@ashd.svnit.ac.in

Abstract

Fluorescent N-doped carbon dots (CDs) were derived from dried shrimps and rationally fabricated as a traceable drug delivery system for the targeted delivery of boldine in human breast cancer cell (MCF-7 cells). The CDs served as fluorescent carriers for simultaneous tracking of the carrier and of drug release. The boldine release is triggered upon acidification of the intracellular vesicles, where the carriers are located after their uptake by cancer cells. Further, boldine-loaded fluorescent CDs enhanced their uptake by cancer cells. The MCF-7 cells were used to evaluate the anticancer ability of boldine-loaded CDs. The synthesized blank CDs were used as fluorescent probes for imaging of SH-SY5Y (Human neuroblastoma) cells, which have potential applications in bioimaging and related fields. These results demonstrated that the feasibility of using CDs as traceable drug delivery system with the ability for the delivery of boldine drug into the target cells.

Keywords: Fluorescent CDs, Boldine, MCF-7 cells, Prawn shrimp, FT-IR, UV-visible and fluorescence spectroscopic techniques.

†This work is dedicated to Ms. Stephanie L. D'souza, who was listed as a First co-author, DST- Inspire Ph.D student in the Department of Applied Chemistry, SVNIT from 2012 to 2015, passed away on 3rd May 2015 in Ahmedabad, due to heart stroke.

Introduction

Cancer is a multifactorial molecular disease that includes uncontrolled growth and spread of abnormal cells, has shown tremendous toll on society by causing 1 in 4 deaths in developed countries.[1] It was reported that 14.1 million new cancer cases have been registered in 2012 worldwide, and a figure can be expected to increase to over 22 million cases per year in the next two decades.[2] According to the World Health Organization in November 2014, 8.2 million death cases were occurred from all cancer types, and 32.6 million people living with cancer (within 5 years of diagnosis) in 2012 worldwide.[3] The drug resistance and the severe side effects of chemotherapy are major unresolved issues in clinical oncology. In this connection, novel anticancer compounds with improved features are continuously increasing great interest in chemotherapy.[4-5] Unregulated cell proliferation and resistance to apoptosis are the key responsible for its progression in carcinogenesis, which involves multistage process.[6] Apoptosis (programmed cell death) is the first-line defenses in multicellular organisms to stop tumor development that can be characterized by distinct morphological changes, including cell shrinkage, chromatin condensation, membrane permeability, and disruption of the mitochondrial membrane.[7-8] To explore the drugs targeting apoptotic pathways, various organic molecules including camptothecin, paclitaxel, and doxorubicin have been exploited as anticancer drugs for cancer therapy as well as chemoprevention.[9] These drugs effect by regulating key events or molecules in apoptosis-inducing signal transduction pathways. In order to exploit the potential use of plant-derived compounds as drugs, different alkaloid molecules have been isolated from various plants and used as novel anticancer drugs with reduced side effects. Among these, boldine ((S)-2,9-dihydroxy-1, 10-dimethoxyaporphine) is an aporphine alkaloid and abundantly found in *Peumus boldus* Molina.[10] It exhibits potent antioxidant activity and possesses

hepatoprotective, antitrypanosomal, and anti-inflammatory properties.[11] As a result, cytotoxic effects of boldine have been investigated in bladder carcinoma and glioma cancer cells and studied its antitumor activity in breast adenocarcinoma using *in vitro* and *in vivo* models.[6, 12,13] Although the cytotoxic effects and antitumor activity have already been reported by investigating bladder carcinoma and glioma cancer cells, the boldine delivery studies and its confirmation has not yet to be demonstrated.

In recent years, carbon nanomaterials-based drug delivery systems have shown promising impact in the treatment of cancer due to their drug loading and releasing capacity towards target cells, which results better pharmacokinetics and biodistribution profiles of the drug.[14] Among the carbon nanomaterials, carbon dots are a new type of carbon-based nanomaterial and recognized as the next generation of green and biocompatible nanomaterials with enormous potential as biocompatible imaging probes due to their unique optical properties.[15] Since the surfaces of CDs have different functional blocks with multifunctionality, which impart the attachment of drugs and makes them ideal carrier probes for the simultaneous treatment and tracking of cancer cells.[16] In order to enhance the fluorescence properties of CDs, doping of heteroatoms in CDs is one of promising approach for either enhancing quantum yield or tuning emission wavelength.[17] Among the doping elements in CDs, nitrogen (N) is the most prominent doping atom that can be easily incorporated into the carbon framework, because the nitrogen atom has a comparable atomic size and five valence electrons to bind carbon atoms effectiely.[18] In this connection, various synthetic approaches have been explored to dope nitrogen atom into the carbon framework by using various chemical modifications, such as treatment of carbon materials with ammonia at high temperatures,[19] carbonization of nitrogen containing compounds at high temperature,[20] and polymerization of nitrogen containing compounds in liquid-phase,[21]

respectively. In addition, various organic molecules including aminoacids,[22] streptomycin,[23] ethylenediamine tetraaceticacid,[24] mixture of amines with acid (aniline, ethylene diamine, and phosphoric acid),[25] and various alkylol amines (monoethanolamine, biethanolamine and triethanolamine)[26] as precursors for doping of heteroatoms (N, S and P) in CDs with enhanced fluorescence, high yield and high biocompatibility. Even though hetero atoms were successfully incorporated into the carbon network, all these above-mentioned methods required either extra chemical additives (precursors) or severe synthetic conditions, which limit their wide applications. Thus, the development of simple and low-cost methods for the incorporation of heteroatom into carbon framework is highly desired. This type of doping and functionalization may play key role to improve the properties of the CDs, which extends their potential and/or practical applications. To meet green chemistry guidelines, we selected dried shrimps as precursors for one-step synthesis of N-doped fluorescence CDs without any chemical additives.

In order to explore the potential applications of cell biology, great efforts have been made to develop fluorescent CDs as probes for imaging of bacteria and cancer cells.[27-30] On the other hand, tracking of the drug carriers in living cells is another important issue in drug delivery. In this connection, Mewada and coworkers explored the potential use of sorbitol-derived CDs as drug carriers for targeted delivery of doxorubicin (DOX) to cancer cells.[31] Zhou's group functionalized mesoporous silica NPs with CDs and used as vehicles for delivering of DOX.[32] Matai's group described the use of luminescent CDs with anionic terminus and cationic acetylated G5 poly(amido amine) dendrimers for encapsulation of chemo-drug epirubicin.[33] The negatively charged fluorescent CDs were synthesized using citric acid and *o*-phenylenediamine as precursors and studied their anticancer drug delivery via electrostatic interactions.[34] A facile green synthetic approach was developed for the preparation of DNA-CDs using genomic DNA

isolated from *Escherichia coli* and investigated their drug delivery imaging properties.[35] Similarly, Pandey's group functionalized Au NPs with CDs and used as carriers for delivering of DOX under physiological condition.[36] Karthik's group synthesized a phototrigger conjugated anticancer drug (7-(3-bromopropoxy)-2-quinolylmethyl chlorambucil) and then loaded on the nitrogen-doped CDs for drug delivery.[37] Song and coworkers illustrated the use of fabricated hyaluronic acid on graphene oxide surfaces for controlled release of DOX in tumor therapy.[38] Recently, Capelo et al. functionalized Au NPs with quinoline for sensing of mercury ion and studied their cytotoxicity on the MCF-7 breast cancer cells.[39] The possibility of CDs as a drug delivery vehicle to carry other anticancer-therapeutic agents is explored in the present study.

Herein, we described one-step hydrothermal method for the synthesis of nitrogen-doped fluorescent CDs using dried prawns as precursors. The synthesized CDs were used as potential carriers for effective boldine drug delivery and studied its toxic effects on cancer cells. To this, boldine was loaded on the surfaces of CDs and studied the surveillance of the whole process of internalization, intracellular distribution, and release. The internalizing vesicles will trigger the release of boldine from the CDs, allowing for cell imaging and anticancer drug delivery to MCF-7 cells. The fluorescence of CDs will help in monitoring the drug release process in the cells.

Experimental section

Chemicals

Dried shrimps were purchased from local market in Surat. Boldine was procured from Sigma-Aldrich, USA. Dialysis membrane-70 was procured from HiMedia Laboratories Pvt., India. All the chemicals were used as received without further purification. Water throughout all experiments was obtained by using a Millie-Q water system.

Synthesis of CDs, boldine-loading and releasing on boldine-CDs

The fluorescent CDs were synthesized from dried shrimps through a simple, convenient and one-step hydrothermal method. Briefly, 10 g of dried shrimps were taken into 125 mL of EtOH and 125 mL of water, sealed into a Teflon equipped stainless steel autoclave and then placed in a drying oven followed by hydrothermal treatment at 170 ^{o}C for 12 h. After the reaction, the autoclave was cooled to room temperature. The resulting product was dialyzed against distilled water using a cellulose ester dialysis membrane for 2 days in order to remove impurities from the CDs. A stock solution of boldine (1 mM) was prepared by dissolving 1.6 mg of boldine in 5 mL of EtOH. In order to functionalize CDs with boldine, different volume ratios of CDs and boldine (10:0 and 0:10 v/v) and drug loading efficiency 10 mL of boldine-loaded CDs was dialyzed against deionized water at phosphate buffer silane (PBS) pH 5.2, 7.4 and 9.2. The best volume ratios of boldine and CDs were investigated by UV-visible spectroscopy. The pH-responsive boldine release behavior was studied using UV-visible and fluorescence spectroscopic techniques. The release of boldine from the CDs at pH 5.2, 7.4 and 9.2 were performed as follows: 7:3 mL of boldine-loaded CDs was transferred into a dialysis tube (MWCO ~70 kDa), then the tube was immersed into 40 mL of PBS (pH = 5.2, 7.4 and 9.2) bath at 37°C. At each time point, the outer dialysate was collected and replaced with fresh PBS. Samples were collected at intervals of 180 min for 12 h and then at intervals of 24 h for 3 days. The release of boldine at pH 5.2, 7.4 and 9.2 was analyzed by UV-visible and fluorescence spectroscopic techniques. Cumulative release is expressed as the total percentage of drug released through the dialysis membrane over time using the following formula:

$$[(X_n\text{-}X) / X_n]\times 100$$

Where, X is the fluorescence intensity at 0 hours and X_n is the fluorescence intensity at different hour i.e. X_1, X_2…. n for 3, 6, 9… 60 hour.

Cell culture

The cell culture and imaging experiments were carried out at National Centre for Cell Science, Pune, India. The human breast cancer cell lines (MCF-7) were grown in Dulbecco's Modified Eagle's Medium (Gibco BRL, Carlsbad, CA, USA) supplemented with 10% heat-inactivated fetal bovine serum, and 1% penicillin and streptomycin. The MCF-7 cells were maintained in Dulbecco's Modified Eagle's Medium supplemented with 5% fetal bovine serum, 1% penicillin and streptomycin, 4.5 g/L glucose, 0.005 mg/mL insulin, and 20 mM HEPES. Cells were cultured in tissue culture flasks (Corning, New York, NY, USA) and kept in an incubator at 37°C in a humidified atmosphere with 5% CO_2. For experimental purposes, cells in the exponential growth phase (approximately 70%–80% confluence) were used.

Cell imaging and MTT cell viability assay

For cell imaging, 100 µL of CDs (100 µg/mL) was incubated with MCF-7 and SH-SY5Y (Human neuroblastoma) cells (seeded at 5×10^5 mL^{-1}) for 2 h at 37 ^oC. In another batch, MCF-7 cells were treated with 100 µL of boldine-loaded CDs and subsequently the cells were washed three times with DMSO and the cells then observed after fixing them using paraformaldehyde (2%) and used for imaging.

The cytotoxic effect of blank CDs, free boldine and boldine-loaded CDs was assessed using MTT cell viability assay. The assay was performed for different treatment time points. Briefly, 8.0×10^3 cells were seeded in a 96-well plate and incubated overnight at 37°C in 5% CO_2. On the following day, the cells were treated with blank CDs (100 µg/mL), free boldine

(327.3μg/mL) and boldine-loaded CDs, and incubated further at 37°C in 5% CO_2. The MTT solution was added at 2 mg/mL for 2 hours before addition of dimethylsulfoxide to dissolve the formazan crystals. After this, the medium was replaced with 200 mL of DMSO. This complex was agitated slowly to dissolve the formazan crystals. Finally, the dissolved formazan in DMSO was transferred to fresh 96-well plates and analyzed using a microplate reader (Thermo, USA) at 570 nm. The cell viability was calculated using the following formula (OD, optical density):

Cell viability (%) = $(A_{570}\text{-}A_{630})$ treated cells / $(A_{570}\text{-}A_{630})$ controlled cells × 100

Drug uptake studies

The confocal fluorescence microscopy was used to evaluate the boldine drug uptake studies from boldine-loaded CDs by the MCF-7 cells. First, cells (1×10^5) were seeded on glass coverslips and cultured for 24 hours with normal culture medium. Then, the culture medium was replaced with culture medium containing blank CDs, free boldine and boldine-loaded CDs at boldine concentration of 327.3 μg/mL. After incubation for different times, the glass cover slips were washed three times with PBS, and subjected to fluorescence imaging at excitation wavelengths 405, 488, and 561 nm. The amount of internalised particles in MCF-7 cells was evaluated by the mean fluorescent intensity of blank CDs and boldine-loaded CDs that were internalised by MCF-7 cells.

Instrumentation

Transmission electron microscopy (TEM) image was obtained on a JEOL 2100 transmission electron microscope. Fluorescence spectra were collected using Cary Eclipse Fluorescence Spectrophotometer (Agilent Technologies). The hydrodynamic diameter of the

CDs was measured with a Malvern Zetasizer NanoZS-90 instrument at 25 ^{o}C. UV-visible spectra were obtained on a Maya Pro 2000 spectrophotometer (Ocean Optics, USA). Fourier transform infrared (FT-IR) spectra were recorded on a Perkin Elmer (FT-IR spectrum BX, Germany). The fluorescence lifetimes of the samples were recorded on a Horiba Jobin Yvon IBH Fluorocube instruments after exciting a 370 nm picosecond diode laser. Cell images were measured using a Carl Zeiss 510 LSM laser scanning confocal microscope.

Results and discussion

Characterization of CDs

The fluorescence N-doped CDs were synthesized from dried shrimps by hydrothermal treatment at 170 ◦C for a period of 12 h. The TEM image and size distribution of as-prepared CDs are shown in Supporting Information of Fig. S1. It is revealed that the synthesized CDs are well dispersed in water and in a spherical shape with an average diameter of ~6 nm (Supporting Information of Fig. S2). It can be observed that the CDs consist of carbon, nitrogen, and oxygen, which can be confirmed from the EDX spectra of CDs (Supporting Information of Fig. S2). The elemental analysis shows that the carbon, oxygen and nitrogen weight contents of CDs, implying that the heteroatoms are doped into the CDs. Furthermore, it can also be observed that the other elemental (S and P) peaks were observed in the SEM/EDX spectrum of CDs, indicating that the other elements are also present in the carbon framework. According to the repots,[40-41] elements doping into the CDs improve either fluorescence properties or surface structures of CDs, which facilitates to tune the intrinsic properties of CDs with unexpected non-linear optical properties and applications.[42] Therefore, the presence of other elements may not be effected the fluorescence properties of CDs. Supporting Information of Fig. S3a shows the FT-IR spectrum

of blank CDs. The absorption bands at 1621 and 1402 cm^{-1} correspond to asymmetric and symmetric stretching vibration of carboxyl group. The band at 1675 cm^{-1} is attributed to stretching vibration of C=O groups. The broad bands at 3200–3600 cm^{-1} correspond to bonding vibrations of O-H group, indicating that the prepared CDs exhibit hydrophilicity, which improves their stability and dispersibility in water, without any further surface passivation.[43] The absorption band at 2879 cm^{-1} belongs to $-CH_2$ vibrations in the CDs. The band at 1124 cm^{-1} originates from $-CH_2$ stretching vibration deformation. The characteristic absorption band of the C–O stretching vibration mode was observed at 1047 cm^{-1}. The bands at 1562 and 1477 cm^{-1} are assigned to asymmetric and symmetric bending of primary amines ($-NH_2$), respectively, while the characteristic absorption bands at 3289 and 1337 cm^{-1} belong to the stretching vibrations of N−H and C – N groups. The presence of multifunctional groups (-COOH, -OH, C=O, and NH_2) on the surfaces of CDs demonstrate that the N-doped CDs were derived by decomposing of various organic compounds in dried shrimps, resulting to create a series of emissive traps and to tune emission of CDs with good yield.

Fig. 1 shows the UV-visible absorption and fluorescence emission spectra of as prepared CDs. It can be observed that the absorption maximum shows around 321 nm, which is due to the $\pi \rightarrow \pi^*$ transition of C=C and $n \rightarrow \pi^*$ transition of C=O in the CDs. Fig. 1 displays the fluorescence emission spectrum of as-prepared CDs. It can be seen that the strong fluorescence emission peak centered at 475 nm is recorded under excitation at 430 nm. Importantly, it can also be noticed that the as-prepared CDs have good stability and exhibited blue color under UV illumination (365 nm) (inset) which also displays an excellent aqueous dispersibility. In order to investigate the optical properties of CDs, fluorescence emission spectra of the CDs are measured under various excitations. As shown in Fig. 2, with the increase of excitation wavelength from

350 to 530 nm, emission peaks are red-shifted from 430 (blue) to 543 nm (green), while the fluorescence emission intensities are decreased remarkably, indicating that the excitation-dependent emissions are general feature of CDs. These results indicate that the excitation-dependent fluorescence emission behavior of N-doped CDs is reflected effect from particles of different sizes and a distribution of different surface states of CDs.[39,44] Furthermore, the fluorescence quantum yield of CDs was measured using quinine sulfate as a reference 54%, comparable with those of the reported methods in the literature.[27-29] It is clear that the fluorescence emission intensity of the N doped CDs is strong, and the fluorescence quantum yield of CDs is greatly improved at excitation wavelength of 430 nm. The decay times of N doped CDs in water are similar to those of N-doped CDs in water.[39, 44-46] The fluorescence lifetime (t) of as-prepared CDs was assessed by time-resolved photoluminescence measurements. The fluorescence lifetime of the CDs calculated to be 7.53 ns according to the fluorescence decay profile, with excitation wavelengths of 430 nm and emission wavelengths of 475 nm (Supporting Information of Fig. S4). It can be observed that the CDs exhibit short lifetime, which is indicative of radiative recombination of the excitons.[44, 45]

Study of boldine loading on CDs and its releasing

Loading of boldine on the surfaces of CDs was assessed via UV-visible and fluorescence spectroscopy, taking advantage of the spectral resolution of the absorption and emission peaks CDs as well as absorption spectra of boldine-loaded CDs. Three systems i.e., blank CDs, free boldine and boldine-loaded CDs exhibited characteristic absorption peaks at 307, 321 and 316 nm for blank CDs, free boldine and boldine-loaded CDs (Fig. 3). These results indicated that the boldine is effectively attached on the surfaces of CDs. The amount of loaded boldine was

determined with the help of UV-visible absorption spectra of boldine-loaded CDs at different volumes ratios (boldine:CDs, 0:10 – 10:0 , *v/v*) (Supporting Information of Fig. S5) and the amount of boldine contained within boldine-loaded CDs was 140.3 μg/mL. The fluorescence emission spectra of boldine-loaded CDs were also supported with this conclusion (Supporting Information of Fig. S6). When the boldine-loaded CDs at different volume ratios (0:10 – 10: 0, *v/v*) were excited at 430 nm, there was a drastic changes in the emission spectra at 475 nm corresponding to the CDs (Supporting Information of Fig. S6), indicating that the attachment of boldine on the surfaces of CDs. Similarly, UV-visible absorption spectra of boldine-loaded CDs were drastically changed with varying the volume of CDs and boldine. As a result, the characteristic peaks at 308 (CDs) and 319 nm (boldine) were disappeared and new peaks at 315 nm were observed at bodline and CDs ratios at 7:3 *v/v*, indicating that the successfully loading of boldine on the surfaces of CDs. These results may provide a basis for the simultaneous tracking of the drug carriers on their way into cells and the drug release behavior from the carriers inside the cells.

To confirm the attachment of boldine on the surfaces of CDs, we studied the FT-IR spectra of free boldine and boldine-loaded CDs. As shown in Supporting Information of Fig. S3b, the band at 3099 cm^{-1} corresponds to the sp^3 C-H stretching of boldine. The typical bands at 1499, 1514, 1582 and 1596 cm^{-1} are ascribed to the aromatic C=C stretching. The bands in the range of 1380 to 1470 cm^{-1} are ascribed to aliphatic CH deformation modes. The bands at 1385 and 1468 cm^{-1} represent CH_3 deformation modes. The stretching modes of N–CH_3 group were observed in the range 1274–1415 cm^{-1}. The typical bands at 892, 1015 and 1630 cm^{-1} correspond to–CH bends of aromatic rings, C-N stretching and C=C stretching, respectively. The band at 3398 cm^{-1} corresponds to -OH stretching. Phenolic vibration of boldine was observed at 1206

cm^{-1} while the ether function (CH_3–O–Phe) stretching was observed at 1082, 1132, 1174 and 1239 cm^{-1}, respectively. The medium bands at 771, 813, 869, 892 and 983 cm^{-1} are ascribed to out of plane CH modes. The Phe–OH deformation mode is observed at 6098 cm^{-1} and the band at 564 cm^{-1} is probably ascribed to the deformation mode of the Phe–O–CH_3 moiety. All the observed absorption bands represent the typical molecular signatures of boldine. Supporting Information of Fig. S3c represents the FT-IR spectrum of boldine-loaded CDs, showing following spectral variation, which confirms the interactions of boldine with CDs. The broad band in the range of 3297 - 3427 cm^{-1} corresponds to the intramolecular hydrogen-bonding between CDs and boldine. It can also noticed that the O-H in-plane bending vibration for phenolic groups, in general, lies in the region 1150–1250 cm^{-1} and is not much affected due to hydrogen bonding. The slight shift in the bands at 1458, 1507, 1576 and 1600 cm^{-1} due to the new stretching of aromatic C=C stretching by the interaction of boldine with CDs. The broad peak in the range of 3169 - 3305 indicates that the involvement of amine group of CDs with boldine through hydrogen bonding. These results indicate that boldine is successfully interacted with CDs surfaces by non-covalent interactions.

It was noticed that the cytosol of the cells has a pH value ~ 7.4, whereas the endocytic vesicles, where the particles are entrapped upon internalization, have a lower pH that can reach values of 4.5–5.50.[46] At the same time, *in vivo* applications are envisaged and some tumors are characterized by a slightly more acidic environment than healthy tissue or blood.[47] In this connection, the pH of the solution plays key role on releasing of drug from the surface of nanoparticles, which acts as a trigger for the controlled release of drugs. The boldine-loaded CDs were dialyzed in PBS (pH 5.2, 7.4 and 9.2) for 60 hours to remove unloaded boldine. The percentage release of boldine from the CDs was performed with help of a calibration curve at

various PBS pH conditions (pH 5.2, 7.4 and 9.2), mimicking the environment of intracellular vesicles or of the cytosol, respectively (Fig. 4). At these pH values, there is a continuous release with time and a plateau is reached after 36 hours (Fig. 4). At physiological pH (7.4), the percentage of drug release increases slowly, reaching a maximum value of 84.4 %. At pH 5.2, the percentage of drug release significantly increases with increasing time, reaching a maximum value of 84.8 % after 36 hours and the percentage of the drug release was greater than that of physiological pH 7.4. These can be explained by the following reasons; the hydrophilicity and solubility of boldine are increased at pH 5.2. It was also noticed that the different degree of hydrogen-bonding interaction can be created in between boldine and the CDs under different pH conditions.[48] In acidic conditions, the hydrogen-bonding interactions between the H^+ in the solution and the –COOH, –OH, and $–NH_2$ groups of the CDs and the –OH groups of boldine are weaker than those occurring at neutral pH. At pH 7.4, the phenolic groups of boldine are shown high affinity to interact with the protonated groups of (NH_3^+) the CDs, boldine exhibits negative charge on the phenolic groups of boldine since boldine pK_a value is 6.90,[49] which inhibits the releasing of boldine from the CDs surfaces. These results show that the possibility of using pH as an internal trigger for releasing of boldine drug form the surfaces of the CDs.

As shown in Fig. 3, UV-visible absorption and fluorescence emission spectra of boldine-loaded CDs exhibit different spectral characteristics at different time intervals from 0 to 60 h using a dialysis membrane against buffer solution. Fig. 3a shows the UV-visible absorption spectra of boldine releasing kinetics from the CDs surfaces at different time intervals in pH 5.2. It can be observed that the intensity of absorption peak at 312 was gradually increased with increasing time and reached to maximum at 36 hours. Similarly, the fluorescence emission intensity of the CDs at 491 nm is steadily increasing with increasing time and the percentage of

drug release is reached maximum at 36 hours, confirming that the complete releasing of boldine drug on the surfaces of CDs, which yields to restore the fluorescence emission properties of the CDs (Fig. 3b). Various statistical models including zero order, Primary order, Higuchi model, Hixon–Crowell, Baker–Lonsdale model, Wibull model, Hopenfen burg model, Sequential layer model have been used for the explanation of drug release kinetics. The present boldine drug release mechanism follows Hixon–Crowell model, since the drug release mechanisms may depend on the nature of materials, diameter and surface area varies, which is good agreement with the reported method in the literature using carbon dots as dopamine drug carriers.[50-51] Based on the above results, the CDs act as efficient carriers to accomplish the release and accumulation of drugs in targeted tumor tissues

Biocompatibility and cellular uptake of boldine-loaded CDs

To validate the potential applications and the toxicity of the as-synthesized CDs was evaluated in MCF-7 cells by laser scanning confocal microscopy. Since the objective of the present study was to develop CDs platform to deliver therapeutics to tumors, preliminary studies were carried out to ascertain the suitability of CDs as imaging and delivery probes for MCF-7 cells. As shown in Fig. 5a, the confocal microscopy images of MCF-7 cells incubated with bare CDs for 3 and 48 h at 37 °C. Under 405, 488 and 543 nm excitation, blue, green and red fluorescence of bare CDs in the cell cytoplasm region was observed by using a laser scanning confocal microcopy. The MCF-7 cells showed higher uptake of bare CDs, most of the CDs get into the cell nucleus through nuclear pores, lightening the whole cell. When excited under different wavelengths, blue, green and red photoluminescence was found in the entire cell cytoplasm, indicating that the bare CDs can be effectively taken up by the MCF-7 cells and

mainly localized in the cytoplasm instead of entering the nucleus. The images of MCF-7 cells show different color emissions, which has roots in the excitation dependent luminescence of the CDs. Importantly, the fluorescence intensity of CDs in the cells is almost same even after 48 h (Fig. 5b), indicating that the CDs are stable and exhibited strong fluorescence properties for long time. These results indicate that the CDs show good biocompatibility as bioimaging agents, and act as imaging probes.

The drug delivery capability of boldine-loaded CDs was also investigated by the uptake behavior in MCF-7 cells. Once the uptake of CDs, the localization in acidic vesicles, and the use of pH as a trigger for the release of boldine from the CDs was established, the performance of the CD-based drug delivery system was evaluated *in vitro* in the MCF-7 cell lines. To this, MCF-7 cells were exposed to boldine-loaded CDs at 24 and 48 h. As shown in Fig. 6, very weak fluorescence signals could be observed in the cellular uptake of boldine-loaded CDs at 24 under laser excitations of 405, 488, and 561 nm. Furthermore, the MCF-7 cells incubated with boldine-loaded CDs at 48 h exhibited good fluorescence signals, suggesting that the effective uptake of boldine-loaded CDs by MCF-7 cells through receptor-mediated endocytosis.[31-35] It can be noticed that the blue, green and red fluorescence were clearly visible at 48 h, which is indicative of boldine drug enters into cells quickly via a membrane diffusion pathway and accumulated in the nuclei after incubation. As a result, boldine of boldine-loaded CDs could reach to the nuclei of MCF-7 cells with increasing time, while the CDs are still outside the cell nuclei, suggesting that the boldine is released from boldine-CDs. After 48 hours of incubation, more boldine is distributed in the cell nuclei, indicating that more boldine was released from the boldine-CDs and penetrated into the cell nuclei. These results confirm that the pH-mediated release of drug from entrapped acidic vesicles (where the CDs are) to the cytosol and its diffusion to its target

site, the nucleus, which was beneficial for release of boldine because of the pH sensitive drug release.[46] As a result, non-covalent interactions (hydrogen bonding) can be weakened in the tumor extracellular fluids, which facilitated to release more boldine from boldine-CDs within the cells. Therefore, fluorescence could be observed in the cells due to the cellular uptake of boldine-CDs by the MCF-7 cells via endocytosis, along with gradual intracellular release of boldine from boldine-loaded CDs in the acidic micro-environment of MCF-7 cells. These changes can be enhanced the drug concentration in cells, thereby improving drug cytotoxicity. Therefore, boldine-CDs drug delivery system is steadily released boldine and translocated away from the CDs and moved into the nucleus, indicating that CDs act as ideal carrier probes for the simultaneous treatment and tracking of cancer cells.

In order to prove that as-synthesized CDs as universal imaging probes for all cell lines, the SH-SY5Y (human neuroblastoma) cells uptake of the blank CDs and bioimaging experiments were also performed using a confocal fluorescence microscope *in vitro*. As shown in Fig. 7, the morphologies of SH-SY5Y (human neuroblastoma) cells are almost unchanged before and after incubation with the blank CDs, further confirming their good biocompatibility and low toxicity. It can be clearly observed that the bright blue and green areas inside the SH-SY5Y cells are clearly observed by excitation at 405 and 488 nm, indicating that the CDs are easily internalized into the cells, which suggests that the good stability of the CDs. Notably, the fluorescent spots are observed into the cells, indicating that the CDs are easy to penetrate into the cells but only into the cytoplasm. All of the above results results indicate that the CDs are indeed suitable for long time cell imaging. The excellent biocompatibility (low cytotoxicity) of the CDs guarantees the practical applications for human beings as carriers in drug delivery.

***In vitro* cytotoxicity**

I*n vitro* cytotoxicity studies of blank CDs, free boldine and boldine-loaded CDs were perfomed on the MCF-7 cells by MTT assay. To this, MCF-7 cells are incubated with blank CDs, boldine-loaded CDs and free boldine at 10, 100, 250 and 500 μg/mL for 24, 48, and 72 h, respectively. It can be observed that all formulations of free boldine inhibited the growth of MCF-7 cells in a both time-dependent and dosedependent manner. The blank CDs at 10 μg/mL did not cause obvious cytotoxicity against MCF-7 cells even at 72 h incubation. It was also noticed that the similar cytotoxicity in MCF-7 cells was found for boldine-loaded CDs (10 μg/mL) at 24 h incubation. As a result, the viability of MCF-7 cells after 24 h contact with 10, 100, 250 and 500 μg/mL blank CDs was 104%, 47%, 10% and 6% respectively, whereas the one treated with boldine-loaded CDs was 102%, 24%, 9% and 8% respectively, while the one treated with free boldine drug was 101 %, 8%, 8% and 10% respectively. As shown in Fig. 8, the blank CDs were found to have no obvious effect on the viability of MCF-7 cells. However, the MCF-7 cells were significantly damaged after incubation with boldine-loaded CDs. For a boldine concentration of 327.3 μg mL^{-1}, boldine molecules delivered into the nucleus by boldine-CDs showed more severe cytotoxicity to MCF-7 cells, indicating that boldine-CDs is more readily internalized through the receptor-mediated endocytosis mechanism, while free boldine is transported into cells by a passive diffusion mechanism. As shown in Fig. 8, the boldine-loaded CDs induced death in MCF-7 cells at a comparable rate with free boldine, indicating that the loaded boldine retained its pharmaceutical activity, and caused minimal side effects to the normal cells.

Conclusions

In this work, we report the facile hydrothermal approach for the synthesis of highly fluorescent N-doped CDs using dried shrimps as precursors. The synthesized CDs have multifunctional groups (amino, carboxylic acid and hydroxyl) those can be easily facilitated to load boldine on the surfaces of CDs *via* hydrogen bonding. The fluorescent N-doped CDs act as new fluorescent probes that facilitate simultaneous imaging/mapping of MCF-7 and SH-SY5Y (human neuroblastoma) cells, and as carriers for delivering of boldine drug to the target cells. The multifunctional groups on the CDs provide excellent stability, in addition to attractive fluorescence and extremely high drug loading efficiency. The blank CDs exhibit low cytotoxicity, and only a minute amount is required for effective diagnostic and therapeutic applications. Confocal fluorescence images indicated that the internalization of boldine-loaded by endosomes where boldine is efficiently released and entered the cell nucleus and induced MCF-7 cells death, which is indicative of the effectiveness and selectivity of the drug carrier system. These results demonstrated that the fluorescent N-doped CDs act as fluorescent probes as well as drug carriers for imaging and selective target delivery system, indicating that the biocompatible CDs holds great promise for personal drug delivery with maximal pharmaceutical effects and reduced side effects in chemotherapy.

Acknowledgements

This work is financially supported by the by the Department of Science and Technology, Government of India, India for Inspire Ph.D programme. This work was financially supported by S. V. National Institute of Technology, Surat under Institute Research Grant (Dean (R&C)/1503/2013-2014). We also thank Department of Science and Technology for providing Maya Pro 2000 spectrophotometer under the Fast-Track Young Scientist Scheme (SR/FT/CS-

54/2010). The authors thank Prof. Murthry, Mr. Chetan Patel for the help in the DLS measurements.

References

1. C. E. DeSantis, C. C. Lin, A. B. Mariotto, R. L. Siegel, K. D. Stein, J. L. Kramer, R, Alteri, A. S. Robbins, A. Jemal, *Ca-Cancer J. Clin*. 2014, 64, 252−271.
2. A. B. Chinen, C. M. Guan, J. R. Ferrer, S. N. Barnaby, T. J. Merkel, and C. A. Mirkin, *Chem. Rev*., 2015, 115, 10530−10574
3. World Health Organization; 2014. www.who.int.
4. S. E. Atawodi, *Infect. Agent Cancer*, 2011, **6**, 2-S9.
5. A. Jemal, R. Siegel, E. Ward, T. Murray, J. Xu and M. J. Thun, *CA Cancer J. Clin*.. 2007, **57**, 43–66.
6. M. Paydar, B. Kamalidehghan, Y. L. Wong, W. F. Wong, C. Y. Looi and M. R. Mustafa, *Drug Des. Devel. Ther.,* 2014, **8**, 719–733.
7. R. Scatena, *Adv. Exp. Med. Biol.,* 2012, **942**, 287-308.
8. T. Verfaillie, A. D. Garg and P. Agostinis*, Cancer Lett*., 2013, **332**, 249–264.
9. R. Suzuki, Y. Yasui, H. Kohno, S. Miyamoto, M. Hosokawa, K. Miyashita and T. Tanaka, *Oncol, Rep.,* 2006, **16**, 989–996.
10. H. Speisky and B. K. Cassels, *Pharmacol. Res.,* 1994, **29**, 1–12.
11. P. O'Brien, C. Carrasco-Pozo, and H. Speisky, *Chem. Biol. Interact.*, 2006, **159**, 1–17.
12. D. Gerhardt, A. P. Horn, M. M. Gaelzer, R. L. Frozza, A. Delgado-Cañedo, A. L. Pelegrini, A. T. Henriques, G. Lenz and C. Salbego, *Invest. New Drugs,* 2009, **27**, 517–525.
13. D. Gerhardt, G. Bertola, F. Dietrich, F. Figueirz, A. Zanotto-Filho , J. C. Moreira Fonseca, F.B. Morrone, C.H. Barrios, A. M. Battastini and C. G. Salbego, *Urol. Oncol*., 2014, **32**, 36.e1–36.e9.

14. O. C. Farokhzad and R. Langer, *ACS Nano*. 2009, **3**, 16–20.

15. S. Laurent, D. Forge, M. Port, A. Roch, C. Robic, L. V. Elst and R. N. Muller, *Chem. Rev.,* 2008, **108**, 2064–2110.

16. S. Parveen, R. Misra and S. K. Sahoo, *Nanomedicine: NBM,* 2012, **8**,147–166.

17. L. Li, B. Yu, T. You, *Biosensors and Bioelectronics,* 2015*,* 74, 263–269.

18. Y. Li, Y. Zhao, H. Cheng, Y. Hu, G. Shi, L. Dai and L. Qu, *J. Am. Chem. Soc*., 2011, 134, 15–18.

19. J. Przepiorsi , M. Skrodzewicz , A. W. Morawski, *Appl. Surf. Sci*. 2004, 225, 235 - 242.

20. B. Jurgens , E. Irran , J. Senker , P. Kroll , H. Muller , W. Schnick, *J. Am. Chem. Soc*. 2003, 125, 10288 - 10300.

21. J. S. Lee, X. Wang , H. Luo , G. Baker , S. Dai, *J. Am. Chem. Soc*., 2009, 131, 4596 - 4597.

22. Y. Xu, M. Wu, Y. Liu, X.-Z. Feng, X.-B. Yin, X.-W. He and Y.-K. Zhang, *Chem.–Eur. J*., 2013, 19, 2276–2283.

23. W. Wang, Y. C. Lu, H. Huang, J. J. Feng, J. R. Chen, A. J. Wang, *Analyst*, 2014, 139, 1692–1696.

24. Q. Q. Shi, Y. H. Li, Y. Xu, Y. Wang, X. B. Yin, X. W. He, Y. K. Zhang, *RSC Advances* 2014, 4, 1563–1566.

25. X. Sun, C. Brückner, Y. Lei, *Nanoscale*, 2015, 7, 17278–17282.

26. M. Xu, S. Xu, Z. Yang, M. Shu, G. He, D. Huang, L. Zhang, L. Li, D. Cui, and Y. Zhang, *Nanoscale*, 2015, 7, 15915–15923.

27. V. N. Mehta, S. Jha, S. K. Kailasa, *Mater. Sci. Eng C Mater. Biol. Appl.*, 2014, **38**, 20-27.

28. V. N. Mehta, S. Jha, H. Basu, R. K. Singhal and S. K. Kailasa, *Sensor Actuat. B Chem.,* 2015, **213**, 434-443

29. V. N. Mehta, S. Jha, R. K. Singhal and S. K. Kailasa, *New J. Chem.*, 2014, **38**, 6152-6160

30. B. S. B. Kasibabu, S. L. D'souza, S. Jha, R. K. Singhal, H. Basu and S. K. Kailasa, *Anal. Methods*, 2015, **7**, 2373-2378

31. A. Mewada, S. Pandey, M. Thakur, D. Jadhav and Sharon M, *J Mater. Chem. B*, 2014, **2**, 698–705.

32. L. Zhou, Z. Li, Z. Liu, J. Ren and X. Qu, *Langmuir,* 2013, **29**, 6396−6403.

33. I. Matai, A. Sachdev and P. Gopinath, *ACS Appl. Mater. Interfaces*, 2015, **7**, 11423−11435.

34. B. Wang, S. Wang, Y. Wang, Y. Lv, H. Wu, X. Ma and M. Tan, *Biotechnol Lett.,*2015, 26, 1-11.

35. H. Ding, F. Du, P. Liu, Z. Chen, and J. Shen, *ACS Appl. Mater. Interfaces,* 2015, **7**, 6889−6897.

36. S. Pandey, M. Thakur, A. Mewada, D. Anjarlekar, N. Mishra and M. Sharon, *J. Mater. Chem. B*, 2013, **1**, 4972–4982.

37. S. Karthik, B. Saha, S. K. Ghosh and N. D. Pradeep Singh, *Chem. Commun*., 2013, **49**, 10471—10473.

38. E. Song, W. Han, C. Li, D. Cheng, L. Li, L. Liu, G. Zhu, Y. Song and W. Tan, *ACS Appl. Mater. Interfaces,* 2014, **6**, 11882−11890.

39. C. Núñez, E. Oliveira, J. García-Pardo, M. Diniz, J. Lorenzo, J. L. Capelo and C. Lodeiro, *J. Inorg. Biochem.* 2014, **137**, 115-122.

40. J. Liu, X. Liu, H. Luo and Y. Gao, RSC Adv., 2014, 4, 7648–7654.

41. Y. Chen, Y. Wu, B. Weng, B. Wang, C. Li, Sensors and Actuators B 223 (2016) 689–696.

42. A. Sachev, I. Matai, P. Gopinath, RSC Adv. 4 (2014) 20915.

43. M. Algarra, B.B. Campos, K. Radotic´ , D. Mutavdz˘ic´ , T.J. Bandosz, J. Jiménez-Jiménez, E. Rodriguez-Castellon, J.C.G. Esteves da Silva, J. Mater. Chem. A 2 (2014) 8342.

44. D. Wang, X. Wang, Y. Guo, W. Liu and W. Qin, *RSC Adv.,* 2014, **4**, 51658-51665.

45. Y. Q. Zhang, D. K. Ma, Y. Zhuang, X. Zhang, W. Chen, L. L. Hong, Q. X. Yan, K. Yub and S. M. Huang, *J. Mater. Chem.,* 2012, **22**, 16714-16718.

46. X. Teng, C. Ma, C. Ge, M. Yan, J. Yang and Y. Zhang, *J. Mater. Chem. B*, 2014, **2**, 4631-4639

47. P. R. Gil, M. Nazarenus, S. Ashraf and W. J. Parak, *Small*, 2012, **8**, 943–948.

48. C. Schweiger, R. Hartmann, F. Zhang, W. J. Parak, T. H. Kissel and P. R. Gil, *J. Nanobiotechnology*, 2012, **10**, 28.

49. D. Depan, J. Shah and R. D. K. Misra, *Mat. Sci. Eng. C-Mater*. 2011, **31**, 1305–1312.

50. C. I. Cámara, C. A. Bornancini, J. L. Cabrera, M. G. Ortega and L. M. Yudi, *Talanta*, 2010, **83**, 623-630.

51. M. S. Khand, S. Pandeya, A. Talibd, M. L. Bhaisarea and H. F. Wu*, Colloids Surf. B Biointerfaces*, 2015, **134**, 140–146.

Figure captions

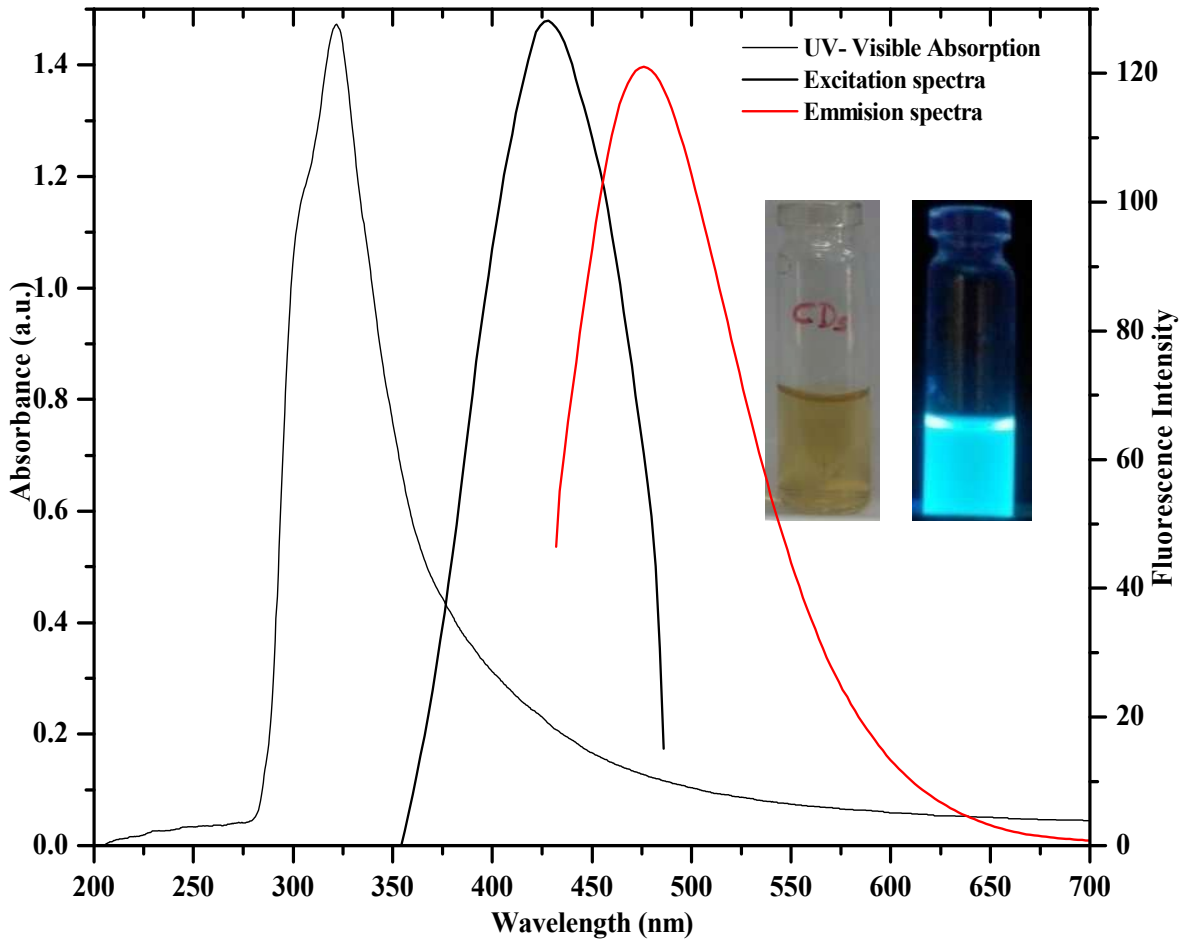

Fig. 1. UV-visible absorption spectrum, fluorescence excitation and emission spectra of CDs when excited at 430 nm and emission (λ_{em} 475 nm). Inset picture shows the CDs under daylight (left) and UV light at 365 nm wavelength (right).

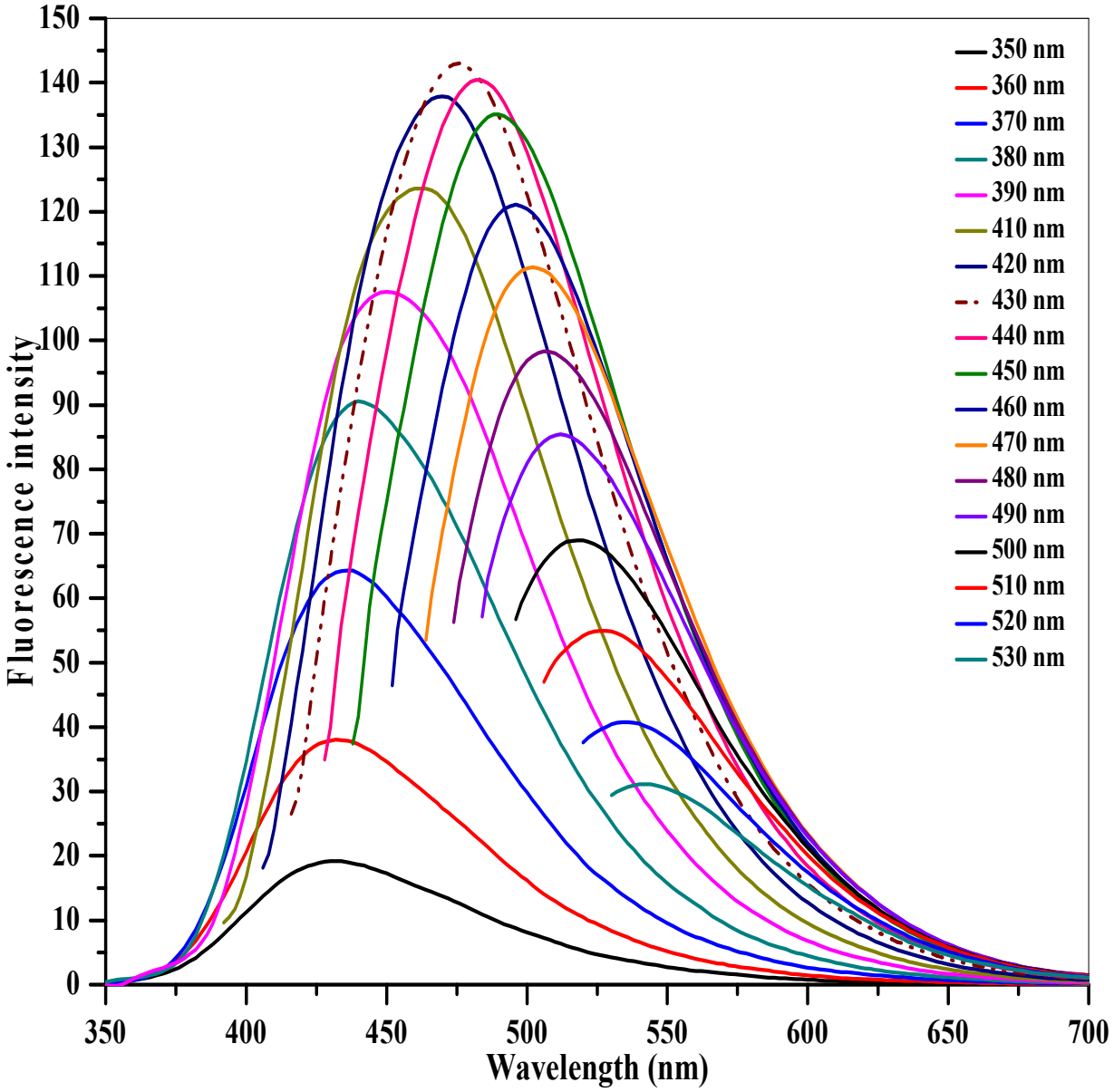

Fig. 2. Emission spectra of carbon dots at different excitation wavelengths from 350 to 530 nm with a progressively increasing 10 nm.

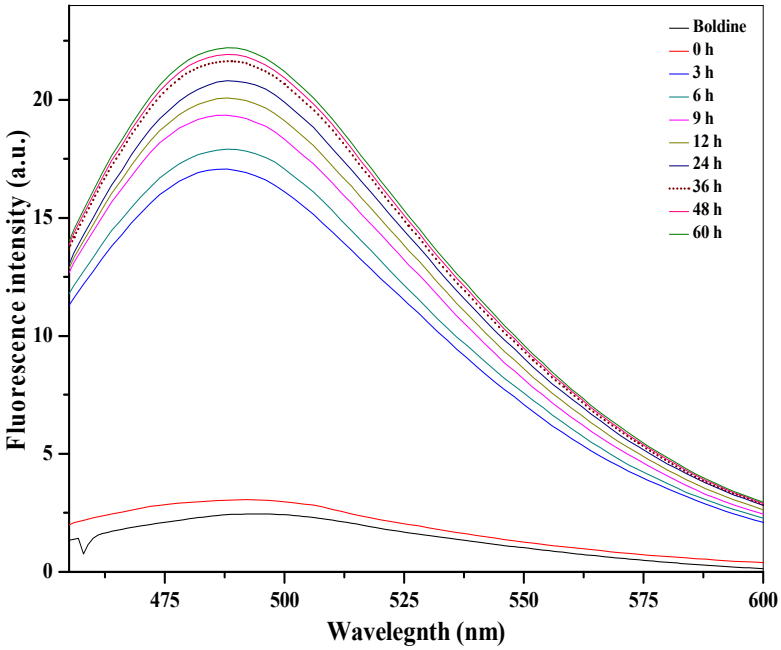

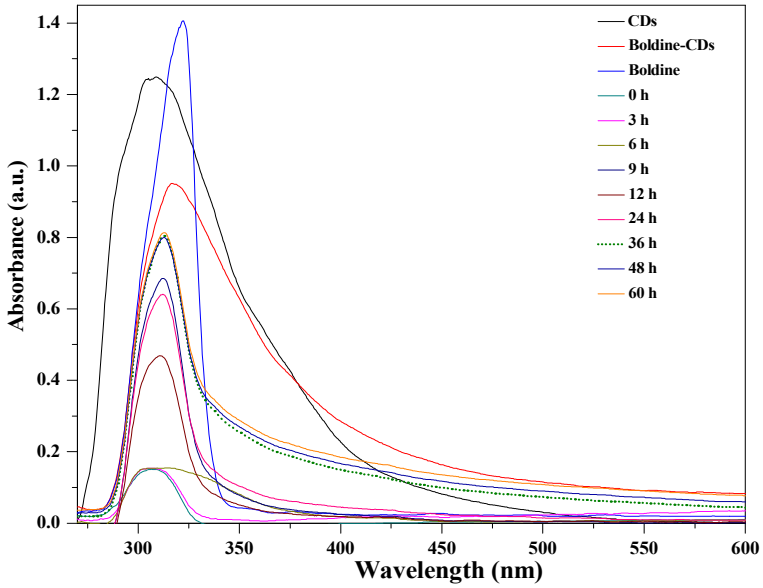

Fig. 3. (a) UV-visible and (b) emission spectra of boldine-loaded CDs at different time intervals from 0 to 60 h in PBS buffer at pH 5.2. Boldine responses of 327.27 µg/mL boldine-loaded CDs under 430 nm excitation.

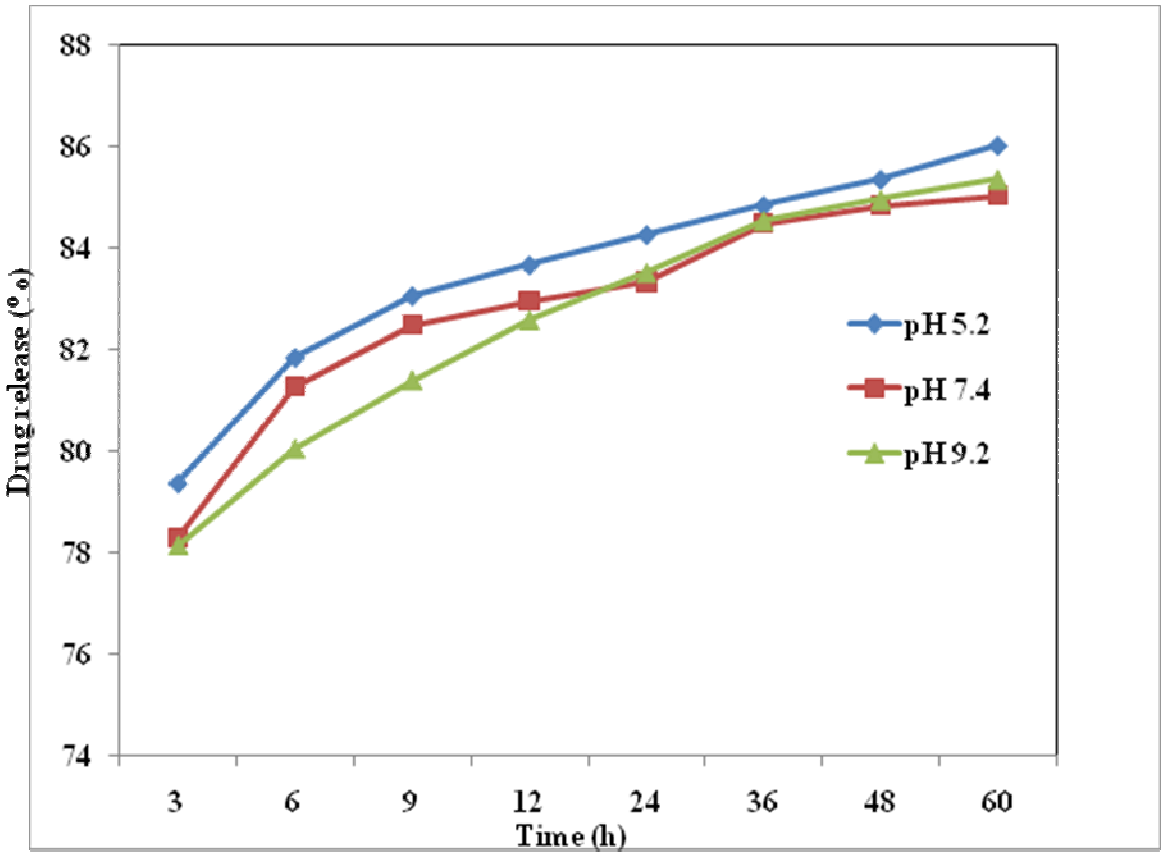

Fig. 4. Boldine drug release (%) from boldine-loaded CDs in PBS with pHs of 5.2, 7.4 and 9.2 at 37 °C.

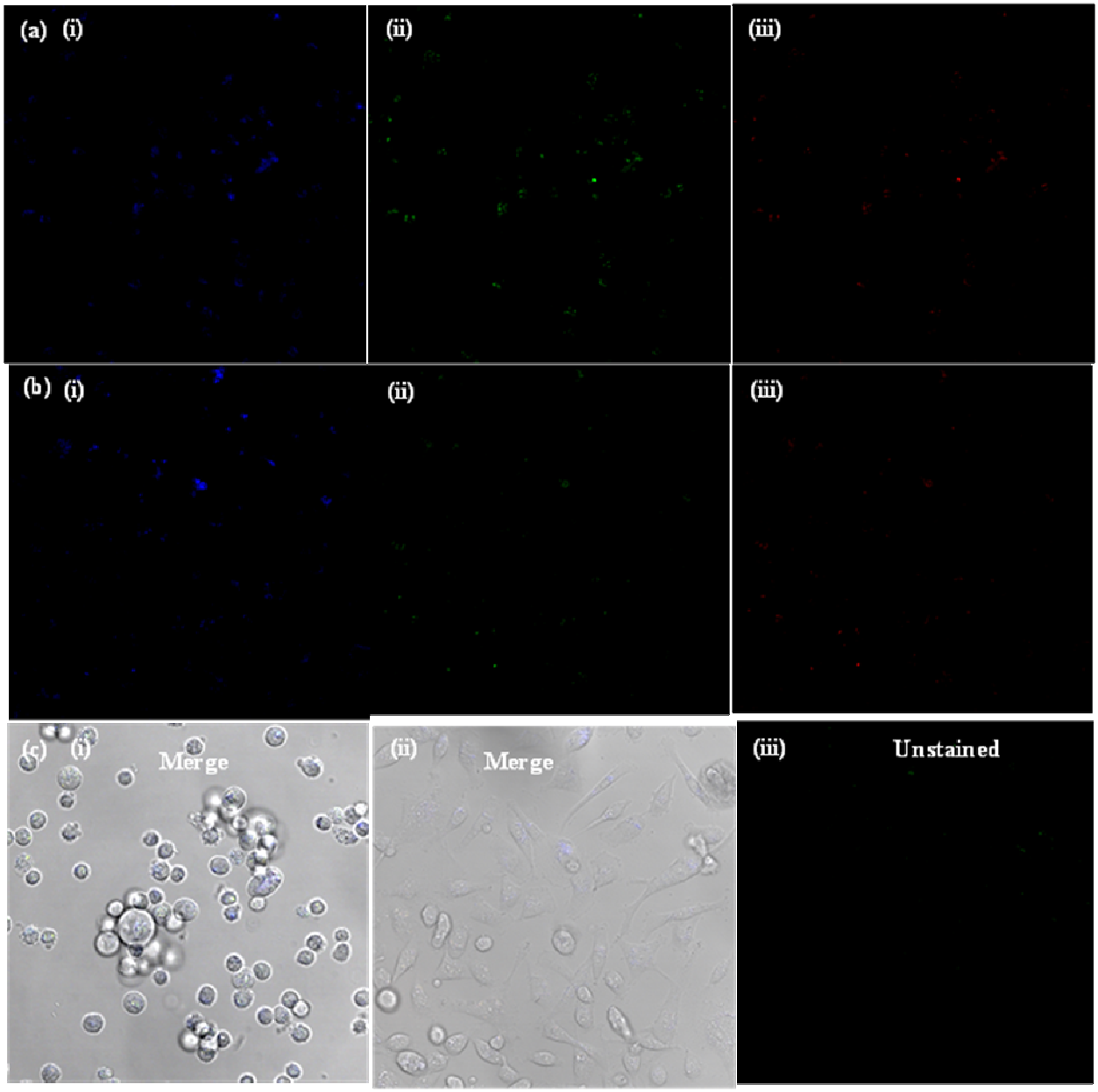

Fig. 5. Localization of bare CDs in MCF-7 cells, and the cells were incubated with bare CDs for (a) 0 and (b) 48 h at 37 °C. The images were obtained under different laser excitation of (i) 405

nm; (ii) 488 nm; (iii) 561 nm, respectively. (c) Localization of bare CDs in MCF-7 cells in merge mode at (i) 0 h, (ii) 48 h and (iii) unstained (without CDs).

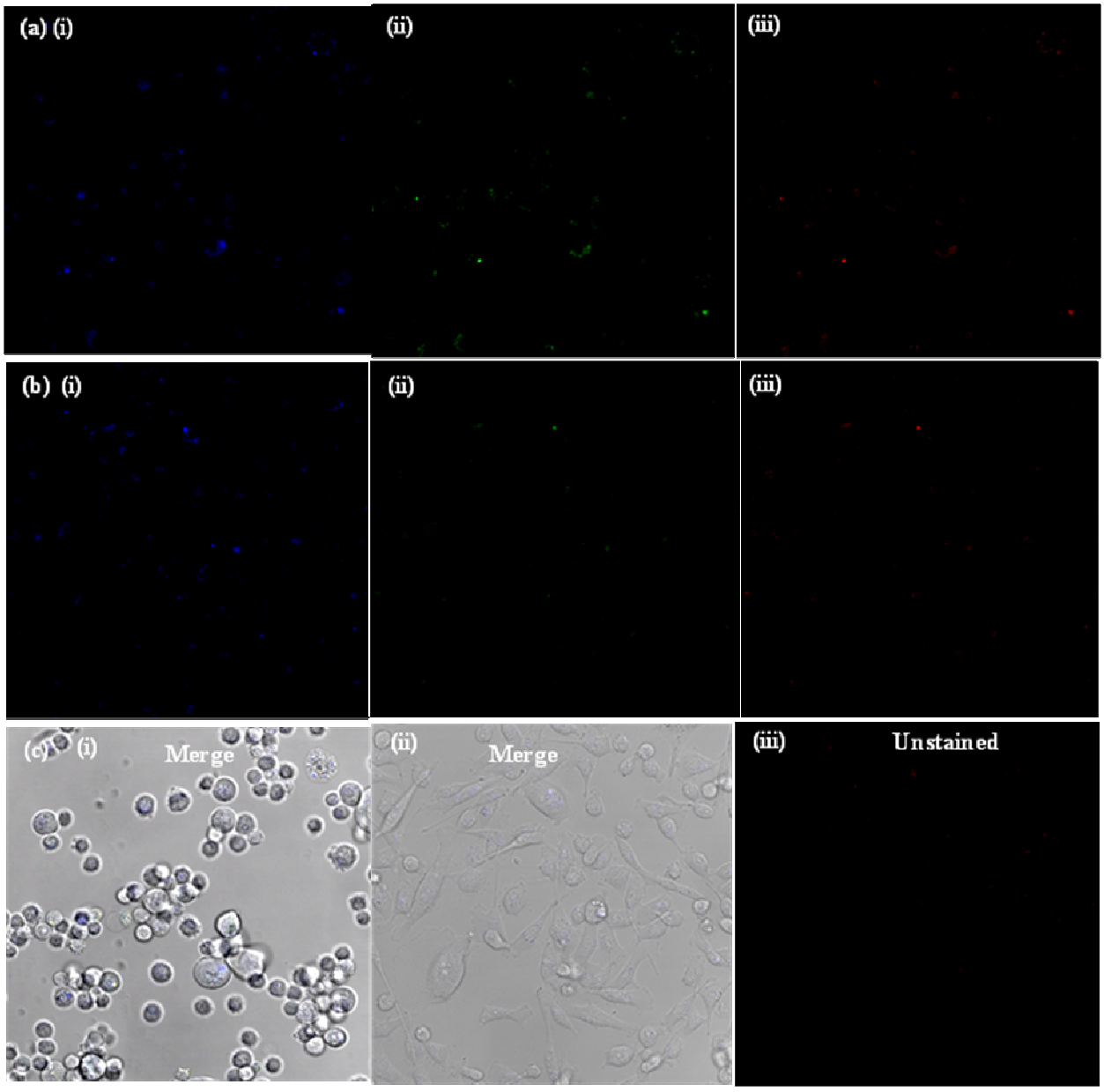

Fig. 6. Laser scanning confocal microscopy images showing the cellular uptake of boldine-CDs at (a) 24 h and (b) boldine-CDs at 48 h by MCF-7 cells, obtained under different laser excitation

of (i) 405 nm; (ii) 488 nm; (iii) 561 nm, respectively. (c) (c) Localization of boldine-CDs in MCF-7 cells in merge mode at (i) 0 h, (ii) 48 h and (iii) unstained (without boldine-CDs).

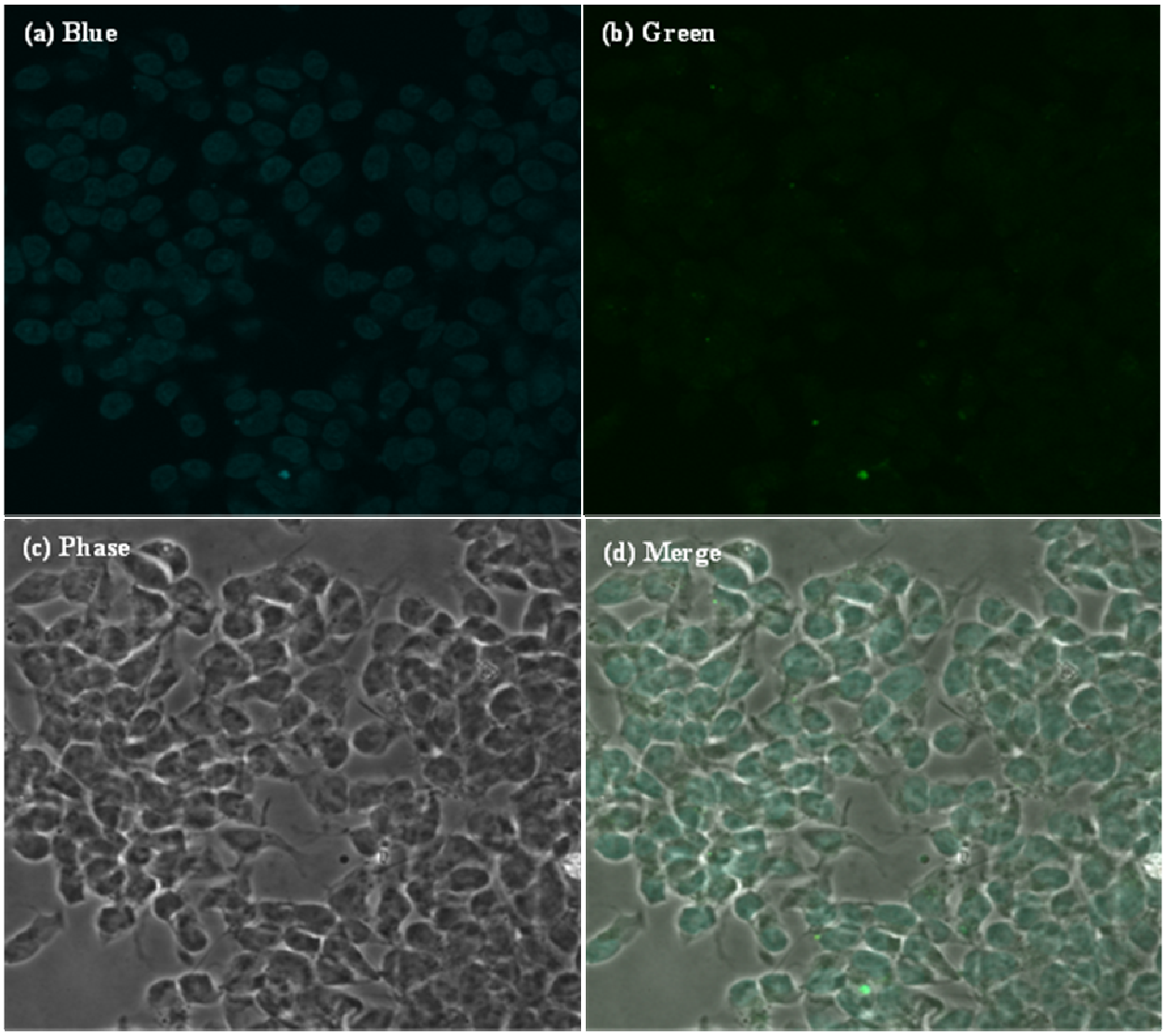

Fig. 7. Laser scanning confocal microscopy images of SH-SY5Y (human neuroblastoma) cells after the cellular uptake of CDs.

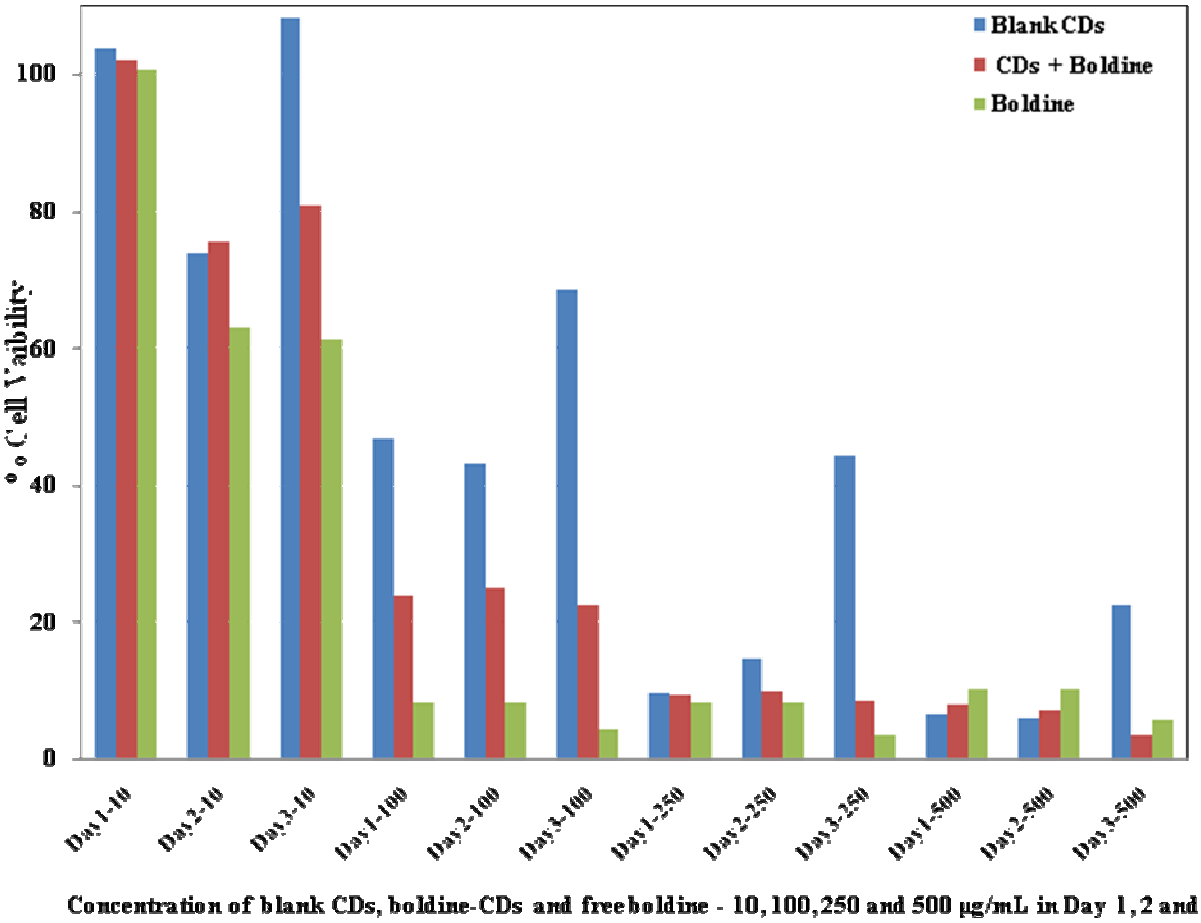

Fig. 8. Relative cell viabilities of MCF-7 cells incubated with blank CDs, boldine-CDs and free boldine at 10, 100, 250 and 500 µg mL^{-1} for 24, 48 and 72 h.

Graphical abstract

The fluorescent N-doped carbon dots (CDs) were synthesized using dried shrimps as precursor and used as carriers for the targeted delivery of boldine to MCF-7 cells. The boldine-loaded CDs enhanced their uptake by cancer cells. Moreover, the synthesized CDs were used as fluorescent probes for imaging of SH-SY5Y (Human neuroblastoma) cells, which have potential applications in bioimaging and related fields.

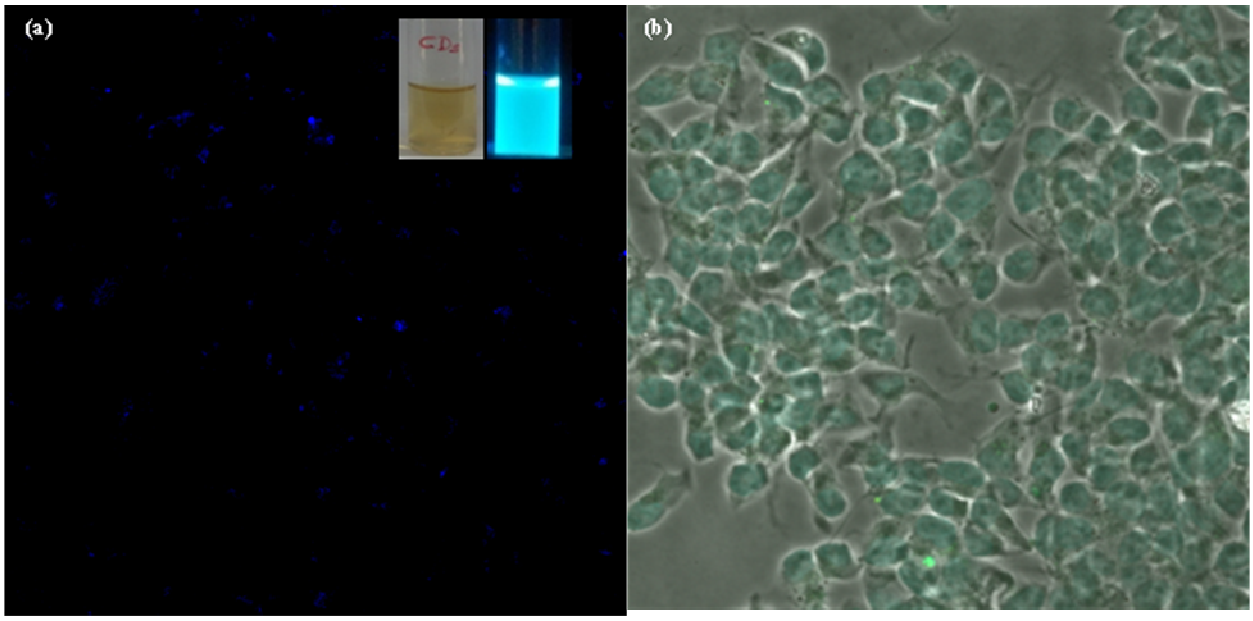

Laser scanning confocal microscopy image showing the cellular uptake of boldine-CDs at 48 h by MCF-7 cells, obtained under different laser excitation of 405 nm. Laser scanning confocal microscopy image of SH-SY5Y cells after the cellular uptake of CDs. Inset: photographic image of CDs under day light and UV light at 365 nm.